

## Eigenfunction expansion solution and finite element solution for orthotropic hollow cylinder under sinusoidal impact load

X. Wang<sup>†</sup> and H. L. Dai<sup>‡</sup>

*Department of Engineering Mechanics, The School of Civil Engineering and Mechanics,  
Shanghai Jiaotong University, Shanghai 200240, P.R. China*

*(Received April 11, 2002, Accepted May 6, 2003)*

**Abstract.** The histories and distributions of dynamic stresses in an orthotropic hollow cylinder under sinusoidal impact load are obtained by making use of eigenfunction expansion method in this paper. Dynamic equations for axially symmetric orthotropic problem are founded and results are carried out for a practical example in which an orthotropic hollow cylinder is initially at rest and subjected to a dynamic interior pressure  $p(t) = -\sigma_0(\sin\alpha t + 1)$ . The features of the solution appear the propagation of the cylindrical waves. The other hand, a dynamic finite element solution for the same problem is also got by making use of structural software (ABAQUS) program. Comparing theoretical solution with finite element solution, it can be found that two kinds of results obtained by two different solving methods are suitably approached. Thus, it is further concluded that the method and computing process of the theoretical solution are effective and accurate.

**Key words:** orthotropic hollow cylinder; impact load; theoretical solution; finite element solution.

---

### 1. Introduction

An orthotropic hollow cylinder under impact pressure can be used in applications involving aerospace, offshore and submarine structures, pressure vessels, and some civil engineering structures. Dynamic stresses in an orthotropic hollow cylinder subjected to interior time - dependent pressures are typical orthotropic elastodynamic problems in which solutions of the orthotropic Navier's equation within a finite cylindrical region under specified initial and Cauchy type boundary conditions should be sought. Practical interesting will be found in a wide range of structure analyses with consideration of the dynamic effects.

The key of above problem lies in obtaining a basic solution for orthotropic dynamic equation with given boundary and initial conditions. In recent years, analyses and calculations for an finite structure under impact load have been studied by means of some methods such as integral transforms (Baker 1961, 1966); Ray theory (Pao 1978, 1983); Finite Hankel transform and Laplace transform (Cinelli 1965, 1966, Wang and Gong 1992, Wang 1993, 1995, Cho 1998) and

---

<sup>†</sup> Professor

<sup>‡</sup> Doctor

Eigenfunction expansion method (Eringen and Suhubi 1975, Gong and Wang 1991, Yin 1997). However, the above studies were most confined to isotropic shell problems or orthotropic shell under thermal impact. If the structure is not isotropic or subjected a dynamic load, the cases so far studied are much fewer because the solving process is more difficult.

This paper investigates the radial sinusoidal impact response of orthotropic hollow thick cylindrical shell by making use of eigenfunction expansion method. The advantage of this method is the ability to provide a closed-form solution that is applicable to a generally orthotropic cylinder of arbitrary thickness under sinusoidal impact load. Formulation for a practical example is that an orthotropic hollow cylinder is initially at rest and subjected to an uniformly distributed impact pressure  $p(t) = -\sigma_0(\sin\alpha t + 1)$ . The histories and distributions of the dynamic stresses are given and the features of the solution that relates to the propagation of the cylindrical wave are discussed. Lastly, a dynamic finite element solution for the same example is also achieved by means of structural software ABAQUS program. Comparing the theoretical solution and finite element solution, we can conclude that the solving method in the paper is valid.

## 2. Orthotropic elastodynamic equation and solution

The geometry and coordinate of orthotropic hollow cylinder is shown in Fig. 1.  $z$ ,  $r$  and  $\theta$  represent, respectively, the axial, radial and tangential variables. Consider that an orthotropic hollow cylinder is subjected to an impact internal and external pressure  $p_1(t)$  and  $p_2(t)$  distributed uniformly over the surface. According to the geometry of hollow cylinder and the property of impact load, the orthotropic elastodynamic problem studied in the paper is considered as axisymmetric. In the case of the elastic properties described, the distribution of stress and displacement depends only on the radial variable  $r$  and the time variable  $t$ . The radial displacement is  $U = U(r, t)$ . Introducing the engineering constants, we can write the generalized Hooke's law as:

$$\begin{aligned}\sigma_r &= C_{11} \frac{\partial U}{\partial r} + C_{12} \frac{U}{r} \\ \sigma_\theta &= C_{12} \frac{\partial U}{\partial r} + C_{22} \frac{U}{r} \\ \sigma_z &= C_{13} \frac{\partial U}{\partial r} + C_{23} \frac{U}{r}\end{aligned}\quad (1)$$

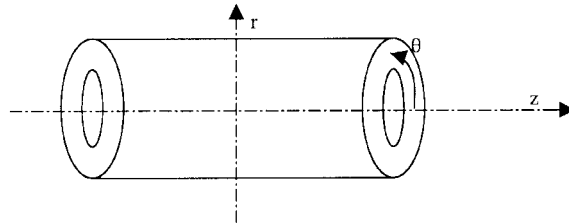


Fig. 1 The geometry and coordinate of orthotropic hollow cylinder

where

$$\begin{aligned}
 C_{11} &= \frac{1}{S} \left( \frac{1}{E_\theta E_z} - \frac{v_{z\theta}^2}{E_z^2} \right), & C_{12} &= \frac{1}{S} \left( \frac{v_{\theta r}}{E_\theta E_z} + \frac{v_{z\theta} v_{zr}}{E_z E_z} \right), \\
 C_{13} &= \frac{1}{S} \left( \frac{v_{\theta r} v_{z\theta}}{E_\theta E_z} + \frac{v_{zr}}{E_\theta E_z} \right), & C_{22} &= \frac{1}{S} \left( \frac{1}{E_r E_z} - \frac{v_{zr}^2}{E_z^2} \right), \\
 C_{23} &= \frac{1}{S} \left( \frac{v_{z\theta}}{E_r E_z} + \frac{v_{\theta r} v_{zr}}{E_\theta E_z} \right), & C_{33} &= \frac{1}{S} \left( \frac{1}{E_\theta E_r} - \frac{v_{\theta r}^2}{E_\theta E_\theta} \right)
 \end{aligned} \tag{2a}$$

$$S = \begin{vmatrix} \frac{1}{E_r} - \frac{v_{\theta r}}{E_\theta} - \frac{v_{zr}}{E_z} \\ -\frac{v_{\theta r}}{E_\theta} \frac{1}{E_\theta} - \frac{v_{z\theta}}{E_z} \\ -\frac{v_{zr}}{E_z} - \frac{v_{z\theta}}{E_z} \frac{1}{E_z} \end{vmatrix} \tag{2b}$$

It is clear that in the case of the elastic properties indicated, the elastodynamic equation in terms of radial displacement  $U(r, t)$  of orthotropic hollow cylinder subjected to arbitrary impact load can be described as

$$\frac{\partial^2 U(r, t)}{\partial r^2} + \frac{1}{r} \frac{\partial U(r, t)}{\partial r} - R^2 \frac{U(r, t)}{r^2} = \frac{1}{C_L^2} \frac{\partial^2 U(r, t)}{\partial t^2} \tag{3a}$$

where  $C_L = \sqrt{C_{11}/\rho}$  and  $\rho$  represent, respectively, wave speed and density, and  $R^2 = C_{22}/C_{11}$ .

The initial distributions of radial displacement and velocity are given by

$$U(r, 0) = U_0(r), \tag{3b}$$

$$U, _t(r, 0) = V_0(r) \tag{3c}$$

The Cauchy type boundary conditions are

$$\sigma_r(a, t) = C_{11} \frac{\partial U(a, t)}{\partial r} + C_{12} \frac{U(a, t)}{r} = p_1(t) \tag{3d}$$

$$\sigma_r(b, t) = C_{11} \frac{\partial U(b, t)}{\partial r} + C_{12} \frac{U(b, t)}{r} = p_2(t) \tag{3e}$$

where  $\sigma_r = \sigma_r(r, t)$  represents radial stress.

The eigenfunction expansion theorem states that the general solution for Eq. (3) (equation (5.17.12) in Eringen and Suhubi 1975) can be expressed as

$$U(r, t) = U_s(r, t) + \sum_{n=1}^{\infty} U_n(r) q_n(t) \tag{4}$$

It should be noted that equation (5.17.12) is correct, but equation (5.17.19) is wrong in Erigen and Suhubi (1975), which was discussed in Gong and Wang (1991).

Substitution of (4) into Eq. (3) shows that if  $U_s(r, t)$  satisfies the field equation

$$\frac{\partial^2 U_s}{\partial r^2} + \frac{1}{r} \frac{\partial U_s}{\partial r} - R^2 \frac{U_s}{r^2} = 0 \quad (5)$$

with the inhomogeneous boundary conditions

$$C_{11} \frac{\partial U_s(a, t)}{\partial r} + C_{12} \frac{U_s(a, t)}{r} = p_1(t)$$

$$C_{11} \frac{\partial U_s(b, t)}{\partial r} + C_{12} \frac{U_s(b, t)}{r} = p_2(t) \quad (6)$$

In which the time variable  $t$  is to be treated as a parameter and if  $U_n(r)$  satisfies the following field equation:

$$\frac{d^2 U_n}{dr^2} + \frac{1}{r} \frac{dU_n}{dr} + \left( k_m^2 - \frac{R^2}{r^2} \right) U_n = 0 \quad (7)$$

with the homogeneous boundary conditions:

$$C_{11} \frac{\partial U_n(a)}{\partial r} + C_{12} \frac{U_n(a)}{r} = 0$$

$$C_{11} \frac{\partial U_n(b)}{\partial r} + C_{12} \frac{U_n(b)}{r} = 0 \quad (8)$$

While the time-dependent function  $q_n(t)$  satisfies the equation

$$\sum_{n=1}^{\infty} [\ddot{q}_n(t) + \omega_n^2 q_n(t)] U_n(r) = -\ddot{U}_s(r, t) \quad (9)$$

with the initial conditions (3b) and (3c). Where a dot denotes differentiation with respect to time, and in Eqs. (7) and (9),  $k_n$  and  $\omega_n$  are, respectively, known as the characteristic values and natural frequencies which is described as

$$\omega_n = k_n C_L \quad (10)$$

Then  $U(r, t)$  in Eq. (4) will satisfy basic Eq. (3a) with the initial conditions (3b,c) and boundary conditions (3d) and (3e). Thus, the expression (4) will exactly be the solution of the present problem, provided the functions  $U_s(r, t)$ ,  $U_n(r)$ , and  $q_n(t)$  have been determined. The process for determination of these functions is as follow:

(a) The quasi-static solution  $U_s(r, t)$  was obtained by Lekhnitskii (1981);

$$U_s(r, t) = \Phi_1(r)p_1(t) + \Phi_2(r)p_2(t) \quad (11a)$$

In the above formula, we have

$$\Phi_1(r) = g_1 r^R + g_2 r^{-R} \quad (11b)$$

$$\Phi_2(r) = g_3 r^R + g_4 r^{-R} \quad (11c)$$

$$g_1 = -g^{R+1} / [(C_{11}R + C_{12})(1 - g^{2R})b^{(R-1)}] \quad (11d)$$

$$g_2 = -g^{R+1}/[(C_{12} - C_{11}R)(1 - g^{-2R})b^{-(R-1)}] \quad (11e)$$

$$g_3 = -g_1g^{-(R+1)} \quad (11f)$$

$$g_4 = -g_2g^{(R-1)}, \quad g = a/b \quad (11g)$$

(b) Determination of  $U_n(r)$  is considered to be an eigenvalue problem.  $U_n(r)$  are named eigenfunctions. In general, there will be an infinite number of natural frequencies  $\omega_n$ , ( $n = 1, 2, \dots$ ), which correspond to the free vibrations of the cylinder. A particular frequency  $\omega_m$  ( $n = m$ ), is associated with a particular mode of  $U_m(r)$  for each  $\omega$  the general solution of Eq. (7) is

$$U(r) = A_1J_R(kr) + A_2Y_R(kr) \quad (12)$$

Where  $J_R$  and  $Y_R$  are the Bessel functions of the first and second kind of order  $R$ ,  $A_1$  and  $A_2$  are arbitrary constants. Substitution of Eq. (12) into Eq. (8) yields a set of homogeneous equation and the condition of nontrivial solutions being existent leads to a transcendental equation

$$J_{Ra}Y_{Rb} - J_{Rb}Y_{Ra} = 0 \quad (13)$$

where

$$\begin{aligned} J_{Ra} &= k J'_R(ka) + h_1 J_R(ka), & J_{Rb} &= k J'_R(kb) + h_2 J_R(kb) \\ Y_{Ra} &= k Y'_R(ka) + h_1 Y_R(ka), & Y_{Rb} &= k Y'_R(kb) + h_2 Y_R(kb) \end{aligned} \quad (14)$$

$$h_1 = C_{12}/(aC_{11}), \quad h_2 = C_{12}/(bC_{11}) \quad (15)$$

Eq. (13) is called a characteristic equation and its positive roots determine the infinite number of the characteristic values  $k_n$  ( $n = 1, 2, \dots, \infty$ ) and in turn the natural frequencies  $\omega_n$  though Eq. (10). For a particular mode of  $U_m$ , solution (12) can be rewriting in the form

$$U_m(r) = A_m C_R(k_m r) \quad (16)$$

where

$$C_R(k_m r) = Y_{Ra} J_R(k_m r) - J_{Ra} Y_R(k_m r) \quad (17)$$

and  $A_m$  is an indeterminate constant multiplier which can be determined by introducing a mode normalization condition. The orthonormal relation of the eigenfunction can be selected as this condition. In the present case it can be written as

$$2\pi \int_a^b U_n(r) U_m(r) r dr = \delta_{mn} \quad (18)$$

where  $\delta_{mn}$  is Kronecker symbol. Substituting of Eq. (16) into Eq. (18) and performing the integration, we arrived at

$$A_m = \{2\pi \int_a^b C_R^2(k_m r) r dr\}^{-0.5} \quad (19)$$

(c) To determine the time-dependent function  $q_m(t)$ , both sides of Eq. (9) are multiplied by  $U_m(r)$  and integrated and the orthonormal relation (18) is used to get an ordinary differential equation with variable  $t$  only

$$\ddot{q}_m(t) + \omega_m^2 q_m(t) = \ddot{Q}_m(t) \quad (20)$$

where

$$Q_m(t) = -2\pi \int_a^b U_s(r, t) U_m(r) r dr \quad (21)$$

The initial conditions for Eq. (20) will be obtained by substituting Eq. (4) into Eqs. (3b) and (3c) and using Eq. (18) and Eq. (21), there upon

$$\begin{aligned} q_m(0) &= 2\pi \int_a^b U_0(r) U_m(r) r dr + Q_m(0) \\ \dot{q}_m(0) &= 2\pi \int_a^b V_0(r) U_m(r) r dr + \dot{Q}_m(0) \end{aligned} \quad (22a,b)$$

The functions  $U_0(r)$  and  $V_0(r)$  in the above equations represent the initial distributions of radial displacement and velocity which is defined in Eqs. (3b) and (3c). Thus, the solution of Eq. (20) under conditions (22) is given by

$$q_m(t) = q_m(0) \cos(\omega_m t) + \frac{1}{\omega_m} \dot{q}_m(0) \sin(\omega_m t) + \frac{1}{\omega_m} \int_0^t \ddot{Q}_m(\tau) \sin[\omega_m(t - \tau)] d\tau \quad (23)$$

Note that expressions of Eq. (16) and Eq. (23) are valid for each term of series in Eq. (4). Thus, substitution of Eqs. (11), (16) and (23) into Eq. (4) completes the formal solution. It should be pointed out that after performing the integration in Eq. (23), from Gong and Wang (1991) the solution (4) is shown as

$$\begin{aligned} U(r, t) &= U_s(r, t) + \sum_{n=1}^{\infty} Q_n(t) U_n(r) + \sum_{n=1}^{\infty} U_n(r) \left[ \alpha_n \cos(\omega_n t) + \right. \\ &\quad \left. \frac{1}{\omega_n} \beta_n \sin(\omega_n t) - \omega_n \int_0^t Q_n(\tau) \sin \omega_n(t - \tau) d\tau \right] \end{aligned} \quad (24a)$$

$$\text{where} \quad \alpha_n = 2\pi \int_a^b U_0(r) U_n(r) r dr, \quad \beta_n = 2\pi \int_a^b V_0(r) U_n(r) r dr \quad (24b)$$

### 3. Practical formula for illustrative examples

Suppose that the orthotropic hollow cylinder is initially at rest and subjected to a sinusoidal interior pressure

$$p_1(t) = -[\sin(\alpha t) + 1] \quad (25a)$$

where  $\sigma_0 = 1$  indicates the unit amplitude of the interior pressure and  $\alpha$  is a factor to show the period of dynamic load. In this case the initial and boundary conditions will be

$$U(r, 0) = V(r, 0) = 0 \quad (25b)$$

$$C_{11} \frac{\partial U(a, t)}{\partial r} + C_{12} \frac{U(a, t)}{a} = -[\sin(\alpha t) + 1] \quad (25c)$$

$$C_{11} \frac{\partial U(b, t)}{\partial r} + C_{12} \frac{U(b, t)}{b} = 0 \quad (25d)$$

The quasi-static solution (11a) may be rewritten in the form:

$$U_s(r, t) = -\Phi_1(r)[\sin(\alpha t) + 1] \quad (26)$$

where  $\Phi_1(r)$  is shown in Eq. (11b).

Substitution of Eqs. (16) and (26) into Eq. (21) yields

$$Q_m(t) = A_m B_m [\sin(\alpha t) + 1] \quad (27)$$

where  $A_m$  is given by Eq. (19) and

$$B_m = 2\pi \int_a^b \Phi_1(r) C_R(k_m r) r dr \quad (28)$$

with the initial conditions (24),  $q_m(t)$  can be reduced from Eqs. (22) and (23) to

$$q_m(t) = Q_m(0) \cos(\omega_m t) + \frac{1}{\omega_m} \dot{Q}_m(0) \sin(\omega_m t) + \frac{1}{\omega_m} \int_0^t \ddot{Q}_m(\tau) \sin[\omega_m(t - \tau)] d\tau \quad (29)$$

Substituting Eq. (27) into Eq. (29), we arrive at

$$q_m(t) = A_m B_m I_m(t) \quad (30)$$

where

$$I_m(t) = \frac{-\alpha^2}{\omega_m^2 - \alpha^2} \sin(\alpha t) + \cos(\omega_m t) + \frac{\omega_m \alpha}{\omega_m^2 - \alpha^2} \sin(\omega_m t) \quad (31)$$

Thus, the solution for the present problem is got by substituting Eqs. (26), (16) and (30) into Eq. (4), we have

$$U(r, t) = -\Phi_1(r)[\sin(\alpha t) + 1] + \sum_{m=1}^{\infty} [A_m^2 B_m I_m(t) U_m(r)] \quad (32)$$

where  $\Phi_1(r)$ ,  $A_m$ ,  $B_m$ ,  $I_m(t)$  and  $U_m(r)$  can be exactly given by Eqs. (11b), (19), (28), (31) and (16) respectively. With the known  $U(r, t)$ , the dynamic stress components will be

$$\begin{aligned} \sigma_r(r, t) &= C_{11} \frac{\partial U}{\partial r} + C_{12} \frac{U}{r}, \\ \sigma_\theta(r, t) &= C_{12} \frac{\partial U}{\partial r} + C_{22} \frac{U}{r}, \\ \sigma_z(r, t) &= C_{13} \frac{\partial U}{\partial r} + C_{23} \frac{U}{r} \end{aligned} \quad (33)$$

#### 4. Dynamic finite element calculation

In this chapter, in order to prove further the validity of the theoretical method and the solving process, a dynamic finite element solution for the same example used in the theoretical solution is also achieved by applying the ABAQUS finite element analysis system.

In this dynamic equation of elastic system, applying the Halmiton principle, the dynamic equation of finite element is written as

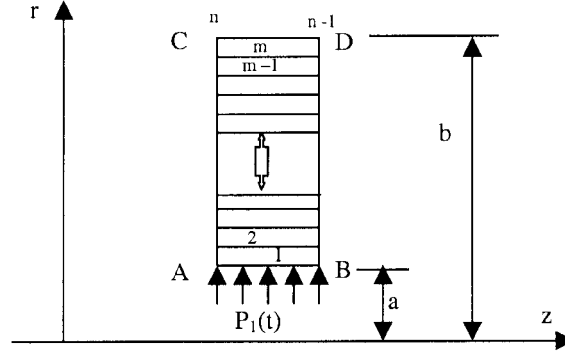


Fig. 2 The element net of the computing model

$$[K]\{d\} + [M]\{\ddot{d}\} = \{F(t)\} \quad (34)$$

where  $[K]$  is the stiff matrix,  $[M]$  is the mass matrix,  $\{d\}$  is the displacement of the knot point and  $\{F(t)\}$  is the dynamic load. In the solving process of the dynamic finite element, applying a direct integral method, the solution of the dynamic Eq. (34) can be obtained. Considering the practical structure shown in Fig. 1 as axisymmetry and plane strain problem, the finite element model and net can be simplified as shown in Fig. 2.

The geometry size and material property are the same as those in the theoretical solution. The finite element net is taken as the axisymmetrically orthotropic rectangular element of 8-knot points. The knot points at AC side and BD side are constrained in the  $z$  direction. In order to make the dynamic finite element solution show a stress wave feature and a strong discontinuity effect at the wavefront, we take 100 elements along radius  $r$  of orthotropic hollow cylinder.

## 5. Results and discussions

Results are carried out in case of  $E_r = E_z = 200 \text{ GP}_a$ ,  $E_\theta = 450 \text{ GP}_a$ ,  $\nu_{\theta r} = \nu_{zr} = 0.25$ ,  $\nu_{z\theta} = 0.167$ ,  $\rho = 5067 \text{ kg/m}^3$ . The dynamic internal pressure  $p_1(t) = -[\sin(\alpha t) + 1]$  is a sudden sinusoidal function load and  $\alpha = 1000$ . Two structures with  $b/a = 20$  and  $b/a = 2$ , are computed and results are shown in Figs. 3 and Figs. 4. In all results, the stresses are normalized by the amplitude of applied pressure  $\sigma_0 = 1$ , the time variable and geometric size are taken as  $T = t^*C_L/a$ , or  $T = t^*C_L/(b - a)$ ,  $R0 = (r - a)/a$ ,  $R1 = (r - a)/(b - a)$ .  $\blacklozenge$  expresses corresponding static stress and  $----$  expresses the solution of the dynamic finite element.

In order to avoid the effects of reflected waves,  $b/a = 20$  and  $t^*C_L/a \leq 20$  are taken. Then the histories of radial, tangential and axial stresses are respectively shown in Figs. 3-1,2,3. The curves in the Figures have clearly shown the features of the compression waves propagating in the orthotropic hollow cylinder upon the application of the interior pressure. The time histories at  $R1 = 1$  and  $R1 = 2$  in Fig. 3-1,2,3 show that before the arrival of the wavefront, dynamic stress is essentially zero, has strong discontinuities at the points where the wavefront arrives at and approaches to the quasi-static solution. Figs. 3-4,5,6 show the distributions of the radial, tangential and axial stresses along the radius  $r$ , in different time. It is clear that the distribution of the dynamic stresses

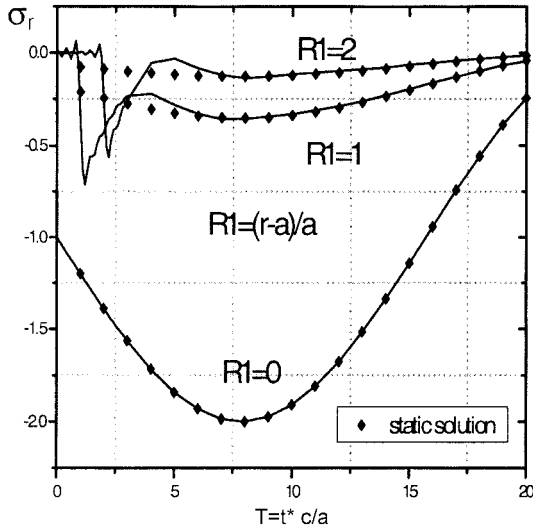


Fig. 3-1 The histories of the radial stress in an orthotropic hollow cylinder under sinusoidal impact load.  $b/a = 20$

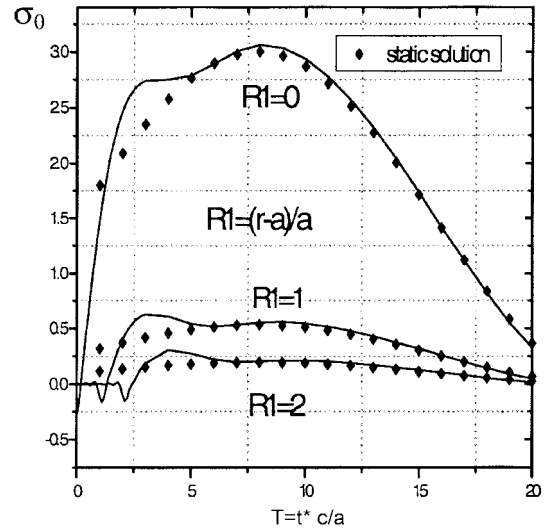


Fig. 3-2 The histories of the tangential stress in an orthotropic hollow cylinder under sinusoidal impact load.  $b/a = 20$

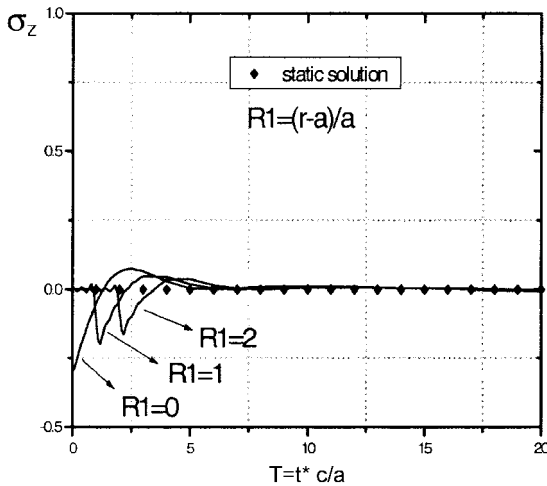


Fig. 3-3 The histories of the axial stress in an orthotropic hollow cylinder under sinusoidal impact load.  $b/a = 20$

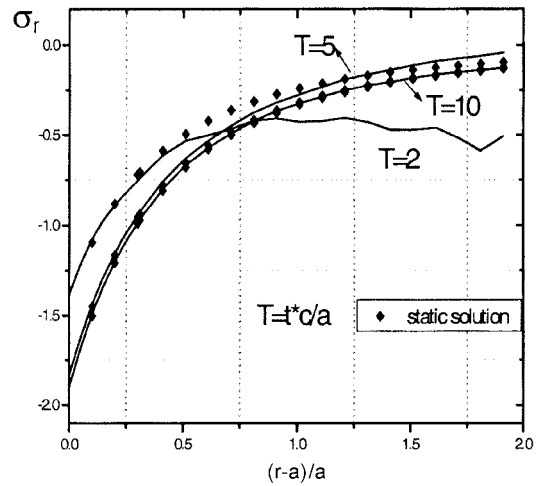


Fig. 3-4 The distributions of the radial stress in an orthotropic hollow cylinder under sinusoidal impact load.  $b/a = 20$

approaches to that of the static stresses when time is large.

Figs. 4 give the computing results of an orthotropic hollow cylinder with  $b/a = 2$ . Because of the small thickness, the effects of wave reflected between the inner wall and outer wall on dynamic stresses must be considered. Except the radial stress at inner boundary  $R1 = 0$  where  $p_1(t) = -[\sin(\alpha t) + 1]$  as shown in Fig. 4-1, the stresses at other points oscillates dramatically around the static stress. Fig. 4-1 shows that the history of the radial stress at inner boundary is strictly

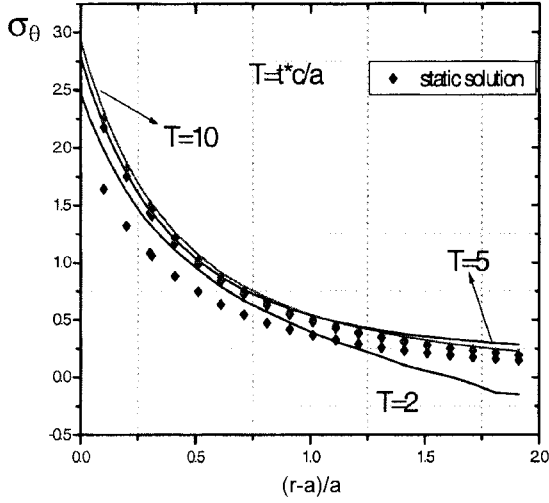


Fig. 3-5 The distributions of the tangential stress in an orthotropic hollow cylinder under sinusoidal impact load.  $b/a = 20$

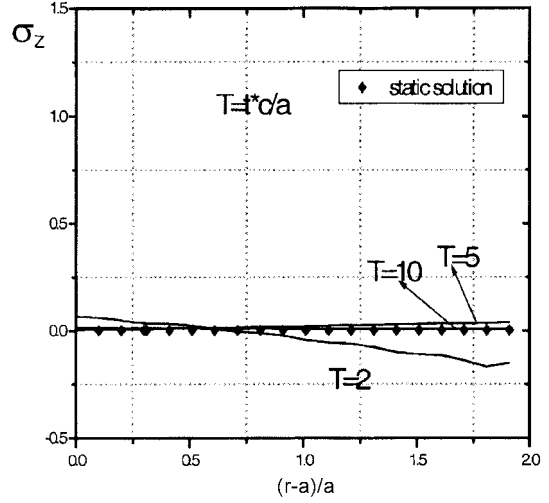


Fig. 3-6 The distributions of the axial stress in an orthotropic hollow cylinder under sinusoidal impact load.  $b/a = 20$

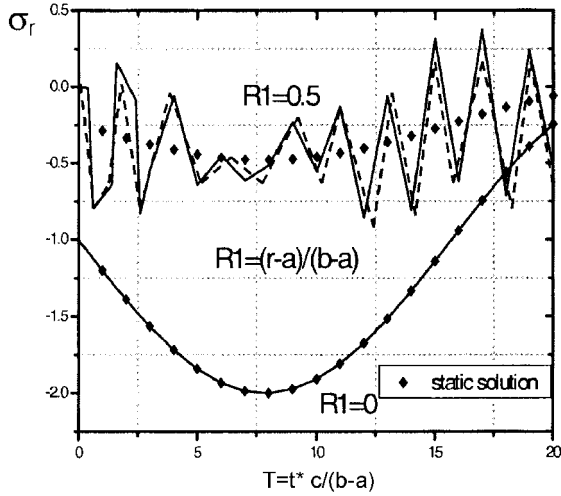


Fig. 4-1 The histories of the radial stress in an orthotropic hollow cylinder under sinusoidal impact load,  $b/a = 2$ . --- represents finite element solution

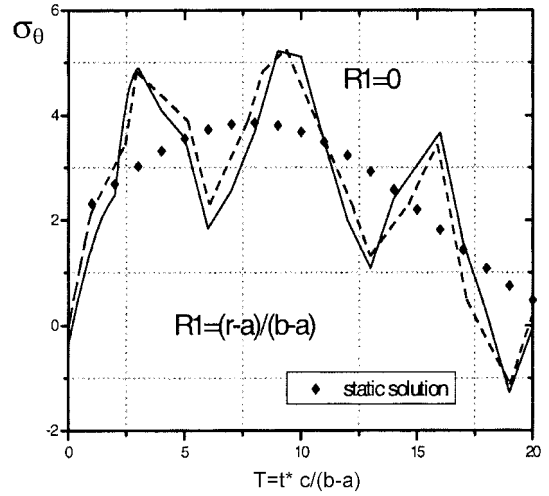


Fig. 4-2 The histories of the tangential stress in an orthotropic hollow cylinder under sinusoidal impact load.  $b/a = 2$ . --- represents finite element solution

coincident with that of the interior pressure  $p_1(t)$ . Thus, the boundary conditions (6) are satisfied. At the middle point  $R1 = 0.5$ , the radial stress oscillates dramatically as shown in Fig. 4-1. The oscillations are accompanied with the stress waves propagating between the boundaries of  $r = a$  and  $r = b$  where the reflected waves are produced successively upon the arrival of the incident wave.

The histories of tangential and axial stresses are shown in Fig. 4-2 to Fig. 4-5 respectively. It

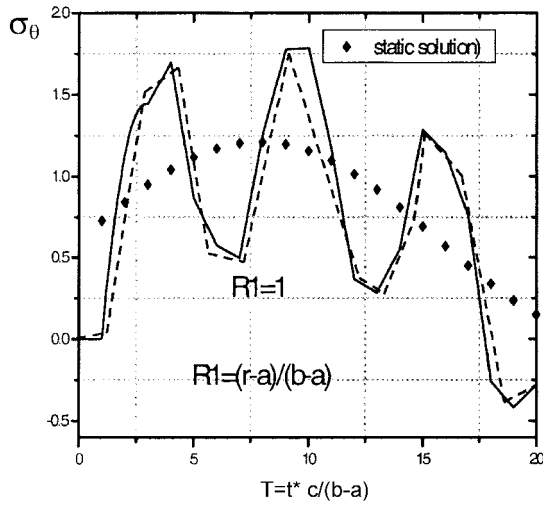


Fig. 4-3 The histories of the tangential stress in an orthotropic hollow cylinder under sinusoidal impact load.  $b/a = 2$ . --- represents finite element solution

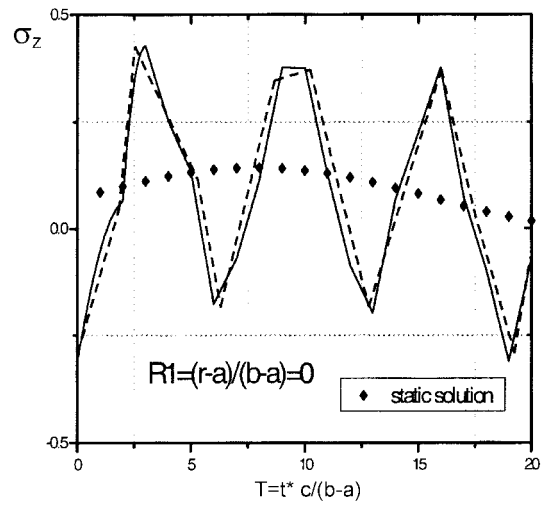


Fig. 4-4 The histories of the axial stress in an orthotropic hollow cylinder under sinusoidal impact load.  $b/a = 2$ . --- represents finite element solution

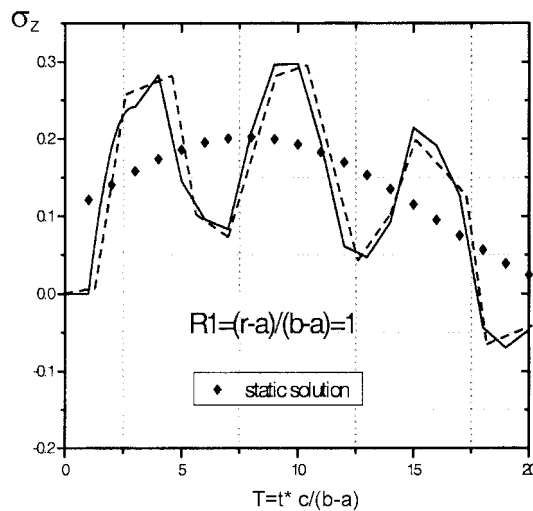


Fig. 4-5 The histories of the axial stress in an orthotropic hollow cylinder under sinusoidal impact load.  $b/a = 2$ . --- represents dynamic finite element solution

should be mentioned that the maximum amplitude of the tangential stress at  $r = a$  is much larger than that of the radial stress.

Lastly, a dynamic finite element solution for the orthotropic hollow cylinder where  $b/a = 2$  is also achieved by means of structural software ABAQUS. The finite element solution obtained is shown in Figs. 4. Comparing the theoretical solution and finite element solution, we can find the results from two kinds of different methods being very approach.

It is concluded from above analyses and results, that eigenfunction expansion solution for orthotropic hollow cylinder under impact load  $p_1(t) = -[\sin(\alpha t) + 1]$  is effective to solve other dynamic problem.

## Acknowledgements

The authors thank the referees for their valuable comments.

## References

- Baker, W.E. (1961), "Axisymmetric modes of vibration of thin spherical shell", *J. Acoust. Soc. Am.*, **33**, 1749-1758.
- Baker, W.E., Hu, W.C.L. and Jackson, T.R. (1966), "Elastic response of thin spherical shell to axisymmetric blast loading", *J. Appl. Mech.*, ASME, **33**, 800-806.
- Cho, H., Kardomateas, G.A. and Valle, C.S. (1998), "Elastodynamic solution for the thermal shock stresses in an orthotropic thick cylindrical shell", *J. Appl. Mech.*, **65**, 184.
- Cinelli, G. (1965), "An extension of the finite Hankle transform and application", *Int. J. Engng. Sci.*, **3**, 539-550.
- Cinelli, G. (1966), "Dynamic vibrations and stresses in elastic cylinders and spheres", *J. Appl. Mech.*, ASME, **33**, 825-830.
- Eringen, A.C. and Suhubi, E.S. (1975), *Elastodynamics*. (Vol. 2, Linear Theory), Academic press. New York.
- Gong, Y.N. and Wang, X. (1991), "Radial vibrations and dynamic stresses in elastic hollow cylinder", In *Structural Dynamic: Recent Advances*. Elsevier Science Publication Ltd. Oxford.
- Lekhnitskii, S.G. (1981), *Theory of Elasticity of an Anisotropic Body*, Mir Publishers Moscow.
- Pao, Y.H. and Ceranoglu, A.N. (1978), "Determination of transient responses of a thick-walled spherical shell by the ray theory", *J. Appl. Mech.*, ASME, **45**, 114-122.
- Pao, Y.H. (1983), "Elastic wave in solids", *J. Appl. Mech.*, ASME, **50**, 1152-1164.
- Wang, X. and Gong, X.N. (1992), "An elastodynamic solution for multilayered cylinders", *Int. J. Engng. Sci.*, **30**(1), 25-33.
- Wang, X. (1993), "Stress wave propagation in a two layered cylinder with initial interface pressure", *Int. J. Solids Struct.*, **30**(12), 1693-1700.
- Wang, X. (1995), "Thermal shock in a hollow cylinder caused by rapid arbitrary heating", *J. Sound Vib.*, **183**(5), 899-906.
- Yin, X.C. (1997), "Multiple impacts of two concentric hollow cylinders with zero clearance", *Int. J. Solids Struct.*, **34**(35), 4597-4616.